Gfi1 integrates progenitor versus granulocytic transcriptional programming

*Shane R. Horman,[1] *Chinavenmeni S. Velu,[1] Aditya Chaubey,[1] Tristan Bourdeau,[1] Jinfang Zhu,[2] William E. Paul,[2] Brian Gebelein,[3] and H. Leighton Grimes[1]

[1]Divisions of Immunobiology, and Experimental Hematology and Cancer Biology, Cincinnati Children's Hospital Medical Center, OH; [2]National Institute of Allergy and Infectious Diseases (NIAID), National Institutes of Health (NIH), Bethesda, MD; and [3]Division of Developmental Biology, Cincinnati Children's Hospital Medical Center, OH

In patients with severe congenital neutropenia (SCN) and mice with growth factor independent-1 (Gfi1) loss of function, arrested myeloid progenitors accumulate, whereas terminal granulopoiesis is blocked. One might assume that Gfi-null progenitors accumulate because they lack the ability to differentiate. Instead, our data indicate that Gfi1 loss of function deregulates 2 separable transcriptional programs, one of which controls the accumulation and lineage specification of myeloid progenitors, but not terminal granulopoiesis. We demonstrate that Gfi1 directly represses *HoxA9*, *Pbx1*, and *Meis1* during normal myelopoiesis. *Gfi1*$^{-/-}$ progenitors exhibit elevated levels of HoxA9, Pbx1 and Meis1, exaggerated HoxA9-Pbx1-Meis1 activity, and progenitor transformation in collaboration with oncogenic K-Ras. Limiting *HoxA9* alleles corrects, in a dose-dependent manner, in vivo and in vitro phenotypes observed with loss of Gfi1 in myeloid progenitor cells but did not rescue *Gfi1*$^{-/-}$ blocked granulopoiesis. Thus, Gfi1 integrates 2 events during normal myeloid differentiation; the suppression of a HoxA9-Pbx1-Meis1 progenitor program and the induction of a granulopoietic transcription program. (Blood. 2009;113: 5466-5475)

Introduction

A hierarchical network of lineage-specifying transcription factors regulates hematopoietic self-renewal, differentiation, survival, and proliferative cell fate decisions; however, the underlying molecular integration of these decisions remains enigmatic. Here, we show that a single transcription factor integrates separable myeloid transcriptional programs governing progenitor biology and terminal differentiation.

The *Hox* genes encode homeodomain proteins that are essential regulators of embryogenesis, hematopoietic development, and transformation.[1] HoxA9 is highly expressed in the hematopoietic stem cell (HSC) fraction of bone marrow,[2] and forced expression of HoxA9 in mouse bone marrow results in enhanced proliferation of pluripotent hematopoietic stem and progenitor cells.[3] In contrast, *HoxA9*$^{-/-}$ mice display a reduction in total leukocytes and lymphocytes and diminished granulocytosis in response to recombinant G-CSF.[4]

HoxA9 forms heterodimeric DNA binding complexes with members of the Pbx and/or Meis family of homeodomain proteins.[5] HoxA9 interactions with Pbx1 increase DNA binding affinity,[6] whereas interactions between Pbx1 and Meis1 may serve to improve nuclear localization.[7] Meis proteins interact with and block the Pbx nuclear export signal, leaving the Pbx nuclear localization signal (NLS) to mediate Pbx nuclear translocation and abundance.[7-9] Similarly, HoxA9 and Meis1 interact without[6] and on DNA.[5] Meis1 interaction mediates HoxA9 nuclear localization, but HoxA9 nuclear retention is regulated by an NLS on either side of the homeodomain.[10] The HoxA9-Pbx1-Meis1 transcription factor complex targets genes involved in HSC and progenitor expansion, including *Pim1*, c-*Myb*, *Cd34*, and *Flt3*.[11-13]

The transcriptional repressor growth factor independent-1 (Gfi1) is a zinc-finger DNA binding protein that is the target of common Moloney murine leukemia virus proviral insertion sites.[14-16] Gfi1 is composed of an N-terminal SNAG transcriptional repressor domain,[17] and a C-terminal Zn-finger domain that is necessary for DNA binding.[18] A single point mutation in the SNAG domain (Gfi1P2A) destroys Gfi1-mediated biology.[17,19-21] Gfi1 is critically required for the development of mature neutrophils,[22,23] and *Gfi1*$^{-/-}$ myeloid progenitors proliferate abnormally.[24] In humans, a GFI1N382S mutation is associated with severe congenital neutropenia (SCN).[25] SCN-associated Gfi1N382S mutations generate a dominant negative-acting protein that is causal in blocking granulopoiesis.[20] Both *Gfi1*$^{-/-}$ mice and patients with GFI1N382S SCN show the abnormal accumulation of arrested myeloid progenitors.[22,23,25]

We recently illustrated direct antagonism between the *Drosophila* orthologs of Gfi1 versus HoxA9, Pbx1, and Meis1.[26] Here, we demonstrate that this relationship extends to mammals. Specifically, Gfi1 directly regulates the expression of the HoxA9-Pbx1-Meis1 transcription factor complex. Moreover, deregulation of Gfi1 increases myeloid progenitor in vitro persistence and in vivo accumulation. Notably, these *Gfi1*$^{-/-}$ phenotypes critically require HoxA9. However, unlike the Gfi1 target gene *Csf1*,[20] modulation of *HoxA9* alleles did not rescue Gfi1 loss-of-function–blocked granulopoiesis. Thus, myeloid progenitor accumulation in both *Gfi1*$^{-/-}$ mice and patients with GFI1N382S SCN correlates with deregulation of HoxA9-directed progenitor transcriptional programs that can be uncoupled from Gfi1-controlled granulopoiesis.

Submitted September 16, 2008; accepted March 29, 2009. Prepublished online as *Blood* First Edition paper, April 3, 2009; DOI 10.1182/blood-2008-09-179747.

The publication costs of this article were defrayed in part by page charge payment. Therefore, and solely to indicate this fact, this article is hereby marked "advertisement" in accordance with 18 USC section 1734.

*S.R.H. and C.S.V. contributed equally to this study.

Methods

Mice

Gfi1$^{\Delta ex4\text{-}5}$ and *Gfi1*$^{fex4\text{-}5}$ mice[27] were backcrossed onto a C57Bl/6 background (The Jackson Laboratory, Bar Harbor, ME). Polymerase chain reaction (PCR) typing of the *Gfi1*$^{fex4\text{-}5}$ allele was performed with primers 5′-CAGTCCGTGACCCTCCAGCAT-3′ and 5′-CTGGGAGTGCACTGCCTTGTGTT-3′, whereas detection of the *Gfi1*$^{\Delta ex4\text{-}5}$ allele was performed with primers 5′-CAGTCCGTGACCCTCCAGCAT-3′ and 5′-CCATCTCTCCTTGTGCTTAAGAT-3′. Data from germline *Gfi1*$^{\Delta ex4\text{-}5/\Delta ex4\text{-}5}$ mice (termed *Gfi1*$^{-/-}$ in the remaining text) are shown throughout the rest of the article; however, essential points were checked with germline *Gfi1*$^{\Delta ex2\text{-}3/\Delta ex2\text{-}3}$ mice[23] and *Gfi1*$^{\Delta ex4\text{-}5/\Delta ex2\text{-}3}$ mice and found to be similar. *Mx-1Cre* transgenic mice were obtained from The Jackson Laboratory. *K-Ras*^{LSLG12D} knock-in mice were obtained from the Mouse Models of Human Cancer repository (National Cancer Institute [NCI], Fredrick, MD). *HoxA7*$^{-/-}$ [28] and *HoxA9*$^{-/-}$ [29] were maintained on C57Bl/6 background. *Rosa-Cre-ER*^{T2} mice[30] were kindly provided by Anton Berns (Netherlands Cancer Institute, Amsterdam, The Netherlands). Mice were bred and housed by Cincinnati Children's Hospital Medical Center (CCHMC) Veterinary Services, and mouse manipulations were reviewed and approved by the Children's Hospital Research Foundation Institutional Animal Care and Use Committee.

Leukemia

The *Mx1Cre*$^{+}$ *LSL-K-Ras*^{G12D} and *Mx1Cre*$^{+}$ *LSL-K-Ras*^{G12D} *Gfi1*$^{fex4\text{-}5/fex4\text{-}5}$ mice were injected intraperitoneally with 100 μg polyinosinic-polycytidylic acid (pIpC) on alternate days for 3 doses. All mice were kept in microisolator cages, were monitored for disease progression every other day initially and every day after the first appearance of symptoms, and were killed when moribund. Statistical analysis was performed using Prism 4 software (GraphPad Software, San Diego, CA). Cumulative survival was plotted against days after treatment with pIpC (log-rank test). Secondary transplantations were performed by injecting 10^6 splenic cells from killed mice into the lateral tail vein of sublethally irradiated (6 Gy) CD45.1 congenic (BoyJ) recipients. Disease progression was monitored as mentioned earlier.

Retroviral constructs

The murine *Gfi1* cDNA was cloned into the *Eco*RI site of the MSCV-IRES-eGFP, SF91-IRES-Venus, and MSCV-Puro retroviral vectors. Gfi1P2A and Gfi1N382S mutants[20] were cloned into the SF91-IRES-Venus vector. Virus stocks were produced by transfecting the Phoenix-Eco packaging cell line.

Bone marrow cell transduction

Bone marrow from 6- to 8-week-old mice was flushed from femurs, tibias, and iliac crests using DMEM (Invitrogen, Carlsbad, CA) with 15% heat-inactivated fetal bovine serum (HyClone Laboratories, Logan, UT) and labeled with mouse Lineage Cell Depletion kit (Miltenyi Biotec, Auburn, CA) followed by separation on an AutoMacs magnetic sorter according to the manufacturer's instructions (Miltenyi Biotec). Cells were maintained in DMEM plus 15% heat-inactivated FBS supplemented with IL-3 (10 ng/mL), IL-6 (20 ng/mL), SCF (25 ng/mL), and TPO (25 ng/mL; all from PeproTech, Rocky Hill, NJ). The cells were expanded in culture for 48 hours before being subjected to retroviral transduction. Briefly, 6-well non-tissue culture–treated plates were coated with RetroNectin (Takara Bio, Kyoto, Japan) according to the manufacturer's protocol and preloaded with viral particles (2-3 MOI/cell). Cells (2×10^6) were plated per well, and spinfected at 1000*g* for 1.5 hours at room temperature, then incubated overnight with the viral supernatants.

In vitro colony assays

Lin$^-$ bone marrow (BM) cells or cells sorted by fluorescence-activated cell sorting (FACS) were plated in methylcellulose medium (M3534; StemCell Technologies, Vancouver, BC) containing IL-3, IL-6, and SCF. Colonies were enumerated and scored after 8 days of culture. For serial replating assays, colonies were pooled, and the number of cells used for the initial plating was replated in fresh methylcellulose medium. *Rosa-Cre-ER*^{T2}*Gfi1*$^{fex4\text{-}5}$ BM cells were plated in methylcellulose media with or without 1 μM tamoxifen.

Real-time quantitative PCR analysis of gene expression

RNA from Lin$^-$ BM cells or sorted cell populations was purified using either Trizol reagent (Sigma-Aldrich, St Louis, MO) or the RNeasy kit (QIAGEN, Valencia, CA). Purified RNA (1-10 μg) was reverse transcribed using the cDNA High Capacity Archive Kit (Applied Biosystems, Foster City, CA) according to the manufacturer's instructions. The reaction products were diluted to 20 ng/μL, and 2 μL was subjected to real-time PCR, which was performed in triplicate using Taqman primer/probe sets on either an ABI Prism 7500 or 7900 amplification system (Applied Biosystems). Taqman primer/probe sets for *c-Myb* (Mm00501741_m1), *CD34* (Mm00519283_m1), *Cxcr4* (Mm01292123_m1), *Ebf1* (Mm00395519_m1), *Flt3* (Mm00439016_m1), *Gfi1* (Mm00515853_m1), *Gfi1b* (Mm00492319_m1), *Hoxa4* (Mm01335255_g1), *Hoxa5* (Mm00439362_m1), *Hoxa6* (Mm00550244_m1), *Hoxa7* (Mm00657963_m1), *Hoxa9* (Mm00439364_m1), *Hoxa10* (Mm00433966_m1), *Hoxa11* (Mm00439360_m1), *Meis1* (Mm00487664_m1), *Meis3* (Mm00485209_m1), *Pbx1* (Mm00435507_m1), *Pbx2* (Mm01134981_g1), *Pbx3* (Mm01333270_m1), *Pim-1* (Mm00435712_m1), *Pu.1* (Mm00488140_m1), and *GAPDH* (Mm99999915_g1; as the endogenous internal control) were purchased from Applied Biosystems.

Morphologic analysis of bone marrow cells

Bone marrow cells were harvested in Medium 199 (Invitrogen) and then briefly lysed in ACK Lysing Buffer (Invitrogen). Cells (n = 50 000) were resuspended in PBS with 0.5% FBS, and cytospins were made with a Shandon EZ Single Cytofunnel (Thermo Electron, Pittsburgh, PA). Slides were disassembled from the funnel and allowed to dry. A HEMA3 stain set (Fisher Scientific, Kalamazoo, MI) was used to perform a hematoxylin-eosin staining on the cells by exposing the slides for 1 minute to each solution. A cover slide was applied with a low-viscosity medium Cytoseal 60 (Richard-Allan Scientific, Kalamazoo, MI). Cells were analyzed on a Zeiss Axiovert 200M microscope (Carl Zeiss, Thornwood, NY) with a 100× objective (Zeiss MicroImaging, Thornwood, NY). Photomicrographs were made with an AxioCam MRc color camera and AxioVision 3.1 software (Carl Zeiss).

FACS analysis of bone marrow cells

Tibias and femurs of mice were harvested and flushed with Medium 199 (Invitrogen) to collect bone marrow cells. Red blood cells were lysed briefly in ACK Lysing Buffer. Bone marrow cells were then incubated in a cocktail of predetermined optimal concentrations of lineage (Lin) antibodies: PE-Cy5–conjugated anti-CD3 (clone CT-CD3), PE-Cy5–conjugated anti-CD4 (clone RM4-5), PE-Cy5–conjugated anti-CD8 (clone 5H10), PE-Cy5–conjugated anti-CD19 (clone 6D5), PE-Cy5–conjugated anti–CD45R-B220 (clone RA3-6B2), PE-Cy5–conjugated anti–Gr-1 (clone RB6-8C5; all from Invitrogen) and PE-Cy5–conjugated anti-TER119 (clone TER119; eBioscience, San Diego, CA). Lin$^+$ cells were then depleted using sheep anti–Rat-IgG (Fc)–conjugated immunomagnetic beads (Invitrogen). Isolated Lin$^-$ cells were stained with PE-conjugated anti-FcRγII/III (clone A7-R34), Pacific Blue–conjugated anti–IL-7Rα (eBioscience), APC-conjugated anti–c-Kit (clone 2B8), FITC-conjugated anti-CD34 (clone RAM34), biotinylated anti–Sca-1 (clone E13-161.7; BD PharMingen, San Diego, CA) and subsequently stained with APC-Cy7–conjugated streptavidin (Invitrogen).

For the analysis of mature myeloid cell populations from whole bone marrow, cells were stained with FITC-conjugated F4/80 (clone CI: A3-1), Alexa-647–conjugated anti-7/4 (clone 7/4; both from AbD SEROTEC, Raleigh, NC), PE-Cy7–conjugated anti–Gr-1 (clone RB6-8C5) and PE-conjugated anti-CD11bα chain (clone M1/70; BD PharMingen). Flow cytometric analyses were conducted on a FACS LSRII (BD Biosciences,

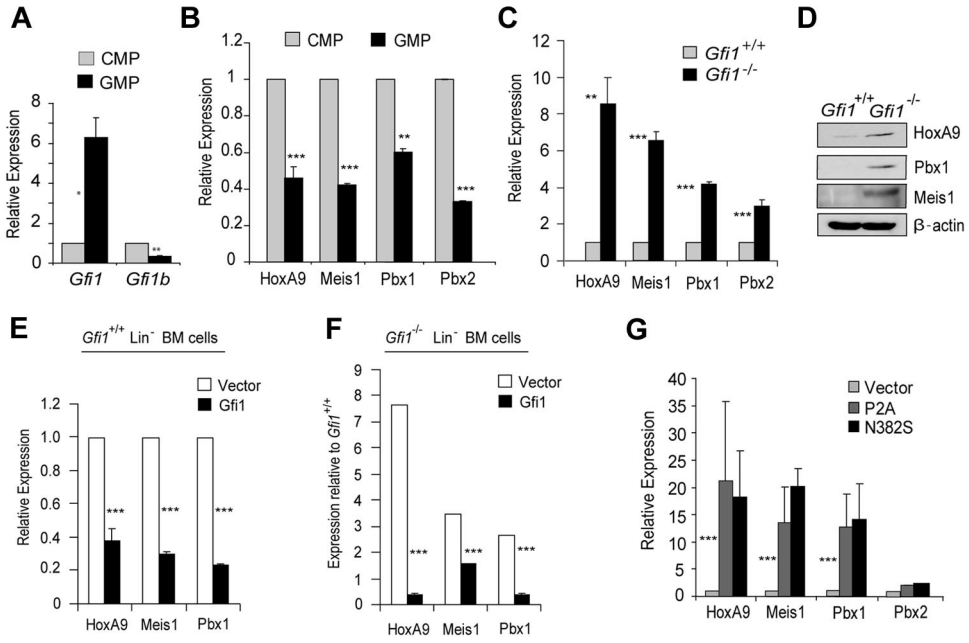

Figure 1. Gfi1 coordinately regulates the expression of the HoxA9-Pbx1-Meis1 complex during myeloid progenitor differentiation. (A) Quantitative real-time gene expression analysis of *Gfi1* and *Gfi1b* in sorted CMPs and GMPs from wild-type Lin$^-$ bone marrow cells. (B) Quantitative real-time gene expression analysis of *HoxA9*, *Meis1*, *Pbx1*, and *Pbx2* in RNA from panel A. (C) Quantitative real-time gene expression analysis of *HoxA9*, *Meis1*, *Pbx1*, and *Pbx2* in RNA from wild-type or *Gfi1*$^{-/-}$ littermate Lin$^-$ bone marrow cells. (D) Immunoblot analysis of HoxA9, Pbx1, and Meis1 in protein extracts from wild-type or *Gfi1*$^{-/-}$ littermate Lin$^-$ bone marrow cells. (E) Quantitative real-time gene expression analysis of *HoxA9*, *Meis1*, and *Pbx1* in RNA from wild-type Lin$^-$ bone marrow cells transduced with an empty retroviral vector (Vector) or 1 expressing Gfi1 (Gfi1). (F) Quantitative real-time gene expression analysis of *HoxA9*, *Meis1*, and *Pbx1* in RNA from *Gfi1*$^{-/-}$ Lin$^-$ bone marrow cells transduced with an empty retroviral vector (Vector) or 1 expressing Gfi1 (Gfi1). (G) Quantitative real-time gene expression analysis of *HoxA9*, *Meis1*, *Pbx1*, and *Pbx2* in wild-type Lin$^-$ bone marrow cells transduced with retrovirus expressing Gfi1 dominant-negative mutants (P2A or N382S) or an empty vector control (Vector). Error bars indicate SD. *$P \leq .05$, **$P \leq .01$, ***$P \leq .001$.

San Jose, CA). Data were exported and analyzed with FlowJo software (TreeStar, Ashland, OR). Statistical analysis from at least 3 independent experiments was performed.

ChIP assays

For chromatin immunoprecipitation (ChIP) analysis, HL60 cells (from Patrick Zweidler-McKay, M. D. Anderson, Houston, TX) were cross-linked with 1% formaldehyde for 10 minutes on ice. Soluble chromatin was prepared using a Bioruptor (Cosmo Bio USA, Carlsbad, CA) to generate DNA fragment size of 200 to 800 bp. Using anti-Gfi1 (2.5D1.7) and control mouse IgG (GE Healthcare, Little Chalfont, United Kingdom) the chromatin-protein complex was immunoprecipitated, and the cross-links were reversed by incubating with NaCl at 65°C for 12 hours. Chromatin was used as input for PCR amplification. The following oligonucleotides were used to amplify the promoter regions to which Gfi1 (and/or HoxA9) binds: *HoxA9* promoter (forward, 5′-CTGTTGGTCGTTTCCGACTT-3′; reverse, 5′-CAAATCGCATTGTCGCTCTA-3′), *Meis1* promoter (forward, 5′-CACTGGCTGGTTGGAGACTT-3′; reverse, 5′-CCCAGACCTC-CATCTCTCAA-3′), *Pbx1* promoter (forward, 5′-GCCGGGAGCCCATT-TCTG-3′; reverse, 5′-CCACTTGGCGAAAAGAAATCAG-3′), *HoxA9* 3′UTR (forward, 5′-TTAAGTGTTCTCGGGGATGC-3′; reverse, 5′-CCG-CATTTTTAAGGTGGAGA-3′), *Meis1* 3′UTR (forward, 5′-GGGCTTGAATT-TGCATGTCT-3′; reverse, 5′-TGCAGTTTTTCCCATCCTTC-3′); *Pbx1* 3′UTR (forward, 5′-TCGAAGCAATCAGCAAACAC-3′; reverse, 5′-GGCTGAAAT-AGCATCCCAAA-3′), *b-actin* (forward, 5′-AGCGCGGCTACAGCTTCA-3′; reverse, 5′-CGTAGCACAGCTTCTCCTTAATGTC-3′).

Immunoblot analyses

Protein extracts were obtained from Lin$^-$ bone marrow cells by lysing cells directly in Complete-M lysis buffer (Roche, Basel, Switzerland). Samples were resolved by 10% SDS–polyacrylamide gel electrophoresis and electrophoretically transferred to PVDF membrane (Immobilon-P; Millipore, Billerica, MA). Immunoblot analysis was performed using the anti-HoxA9 (Upstate Biotechnology, Charlottesville, VA), anti-Pbx1 (Novus Biologicals, Littleton, CO), anti-Meis1 (Abcam, Cambridge, MA) and anti–β-actin (Sigma-Aldrich), and HRP-conjugated goat anti–mouse or anti–rabbit secondary antibody (GE Healthcare) with the ECL-Plus detection kit (Pierce, Rockford, IL).

Results

Gfi1 coordinately regulates the HoxA9-Pbx1-Meis1 complex

Recently, we showed that the *Drosophila* orthologs of Gfi1 (Sensless) and HoxA9 (Abd-B) form a molecular switch antagonizing target gene regulation in embryonic anterior-posterior patterning.[26] We hypothesized that this mechanism of Gfi1-HoxA9 antagonism would be important in mammalian hematopoiesis. Because Gfi1 is known to be critical for granulopoiesis, we examined gene expression in sorted common myeloid progenitors (CMPs) to granulocyte-monocyte progenitors (GMPs). *Gfi1b* (a known Gfi1 target gene that mediates erythroid development) is expressed more in CMPs than in GMPs (Figure 1A). Erythroid potential is much greater in CMPs than in GMPs.[31] Thus, the pattern of *Gfi1b* expression validates the sorted isolation of these populations. *Gfi1* expression is induced during the transition from CMPs to GMPs (Figure 1A). Interestingly, the expression of *HoxA9*, *Meis1*, *Pbx1*, and *Pbx2* is inverse to *Gfi1* expression (compare Figure 1A with Figure 1B). Moreover, we found that HoxA9, Meis1, and Pbx1 mRNA and protein were deregulated in *Gfi1*$^{-/-}$ Lin$^-$ bone marrow cells (Figure 1C,D). Furthermore, this relationship appears to be direct because the forced expression of Gfi1 in *Gfi1*$^{+/+}$ Lin$^-$ bone marrow cells lowered *HoxA9*, *Meis1*, and *Pbx1* transcript levels (Figure 1E), and Gfi1 expression in

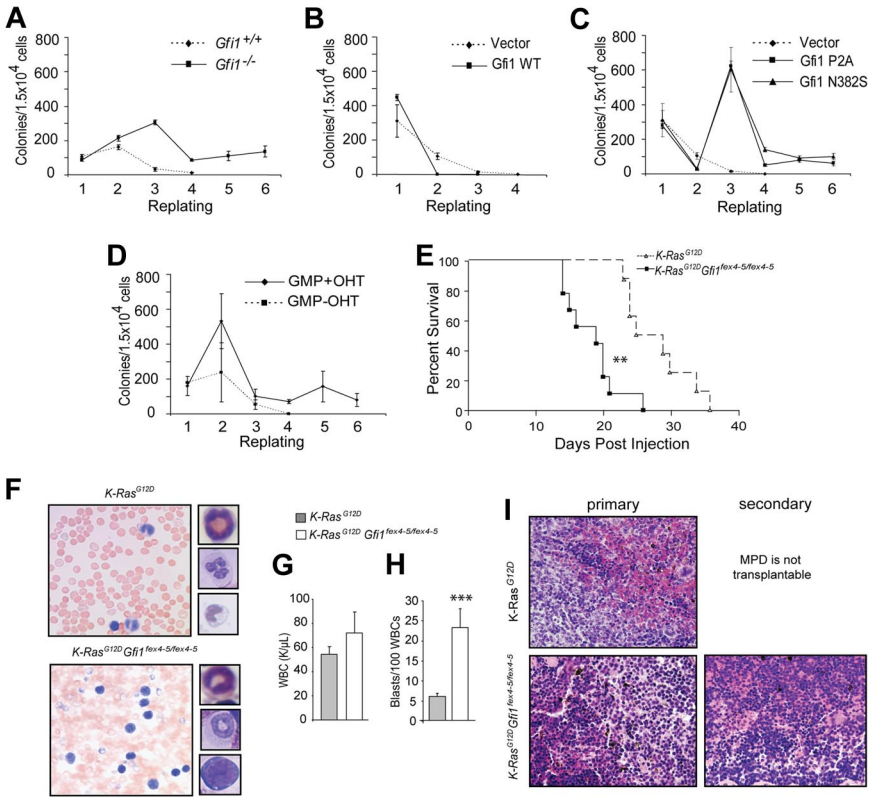

Figure 2. Gfi1 loss of function predisposes to leukemia. (A) Methylcellulose colony-forming assay with serial replating of wild-type and *Gfi1*$^{-/-}$ (*Gfi1*$^{\Delta ex4\text{-}5/\Delta ex4\text{-}5}$) Lin$^-$ bone marrow cells. (B) Methylcellulose colony-forming assay with serial replating of sorted Lin$^-$ wild-type bone marrow cells transduced with retrovirus vectors expressing Gfi1 (Gfi1 WT) or an empty vector control (Vector). (C) Methylcellulose colony-forming assay with serial replating of sorted wild-type bone marrow cells transduced with retrovirus vectors expressing Gfi1 dominant-negative mutants (P2A or N382S) or an empty vector control (Vector). (D) Methylcellulose colony-forming assay with serial replating of *Rosa-CreER*$^{T2+}$ *Gfi1*$^{fex4\text{-}5\ fex4\text{-}5}$ sorted GMPs with or without tamoxifen (OHT) added in vitro to activate the CreER^{T2} protein and delete floxed *Gfi1* alleles. (E) Survival curve of *Mx1Cre*$^+$ *K-ras* ^{lslG12D} (n = 7) or *Mx1Cre*$^+$ *K-ras* ^{lslG12D} *Gfi1*$^{fex4\text{-}5/fex4\text{-}5}$ (n = 7) mice beginning at time of pIpC injections. (F) Photomicrographs (40 ×) of peripheral blood smears from animals upon humane killing from panel E with insets showing myeloid forms and blasts. (G) Peripheral white blood cell (WBC) counts from mice in panel E. (H) Peripheral blood myeloblast counts from mice in panel E. (I) Photomicrographs (5 ×) of H&E-stained splenic tissue from mice in panel E (primary) or recipients of 10^5 spleen cells from moribund *Mx1Cre*$^+$ *K-ras* ^{lslG12D} *Gfi1*$^{fex4\text{-}5/fex4\text{-}5}$ animals in panel E (secondary). Error bars indicate SEM. $^{**}P \leq .01$, $^{***}P \leq .001$.

Gfi1$^{-/-}$ Lin$^-$ bone marrow cells rescued *HoxA9*, *Meis1*, and *Pbx1* expression (Figure 1F). In contrast, forced expression of Gfi1 dominant-negative mutants (Gfi1P2A or Gfi1N382S), which vary from wild type by the mutation of a single amino acid, increased *HoxA9*, *Meis1*, and *Pbx1* transcript levels in wild-type Lin$^-$ bone marrow cells (Figure 1G). We conclude that Gfi1 coordinately regulates the level of HoxA9-Pbx1-Meis1 complex proteins.

Gfi1 loss of function predisposes to leukemia

In mammals, forced expression of HoxA9 in mouse bone marrow results in enhanced proliferation of pluripotent hematopoietic stem and progenitor cells,[3] eventually leading to a fatal, transplantable acute myeloid leukemia (AML).[32,33] Our data indicate that HoxA9 is deregulated onGfi1 loss of function (Figure 1). To determine the biologic sequelae of HoxA9 deregulation in *Gfi1*$^{-/-}$ cells, we performed in vitro and in vivo assays for myeloid progenitor immortalization and transformation.

In vitro, colonies were serially plated past the time when *Gfi1*$^{+/+}$ colony-forming potential was exhausted. Specifically, *Gfi1*$^{+/+}$ and *Gfi1*$^{-/-}$ littermate bone marrow cells were plated in methylcellulose containing stem cell factor, IL-3, and IL-6, and resulting colonies were enumerated. Wild-type cells typically failed to form colonies after the second or third replating. However, cells from *Gfi1*$^{-/-}$ mice consistently formed monocytic-type colonies during 6 serial replatings (Figure 2A). In fact, *Gfi1*$^{-/-}$ CFUs were robust past the 10th replating (data not shown). Next, we forced expression of Gfi1 or Gfi1 dominant-negative mutants[20] and determined the effect on CFU replating capacity. Wild-type Lin$^-$ bone marrow cells were transduced with retrovirus vectors expressing Gfi1 and enhanced yellow fluorescent protein (eYFP). Transduced cells were further expanded for 36 hours, and eYFP$^+$ cells were sorted and plated to assess CFUs. Forced expression of wild-type Gfi1 extinguished all replating capacity (Figure 2B). In sharp contrast, forced expression of Gfi1 dominant-negative mutants gave consistent patterns of CFU during serial platings (Figure 2C). A burst of CFUs was induced in the third plating by both Gfi1P2A and Gfi1N382S, but this was followed by a contraction to a lower number of CFUs that could be replated past that of empty vector transduced cells. This pattern resembles that of CFUs formed by germline *Gfi1*$^{-/-}$ marrow cells during serial plating.

Gfi1 expression is induced during the normal transition between CMPs and GMPs (Figure 1A). We noted that Gfi1 expression inversely correlated with replating ability, because isolated CMPs consistently replated more times than GMPs (data not shown). To provide a molecular link between the level of Gfi1 and GMP colony replating capacity, we used a model in which tamoxifen (OHT)–inducible Cre (*ROSA-Cre-ER*^{T2}) mediates deletion of *Gfi1*$^{fex4\text{-}5}$ alleles in isolated progenitors. On OHT-induced Cre-ER^{T2} activity and *Gfi1* deletion, GMPs consistently generated colonies beyond the sixth plating (Figure 2D), whereas Gfi1-sufficient GMP colony formation was exhausted after the third replating. In fact, Gfi1 deletion allowed for GMP colony formation past the 10th replating (data not shown). To address whether this increase was due to a subset of GMPs with increased replating capacity or whether a gain of function was observed in all cells, we sorted individual GMPs into 96-well plates and monitored their replating ability. A similar percentage of individual GMPs was capable of serial replating compared with the bulk GMP population (data not shown).

Taken together, the high levels of HoxA9, Pbx1, and Meis1, in addition to the abnormally long lifespan of GMPs, suggest that Gfi1-deficient animals may be prone to development of myeloid leukemias. Indeed, forced expression of HoxA9 and Meis1 mediate

leukemogenesis in vivo.[32] That leukemias have not been reported in *Gfi1*$^{-/-}$ mice may be related to the often lethal complications of *Gfi1*$^{-/-}$ phenotypes versus the kinetics of HoxA9-Meis1 leukemogenesis (which extends beyond the lifespan of *Gfi1*$^{-/-}$ mice). To determine whether the Gfi1 null environment is sensitized for leukemia development, we used an established model of myeloproliferative disorder (MPD) and tested the ability of Gfi1 loss of function to progress the disease to leukemia. Oncogenic RAS mutations are among the most frequently detected genetic alterations in patients with AML.[34] However, activation of oncogenic K-Ras^{G12D} in murine bone marrow yields a lethal MPD with short latency and complete penetrance.[35,36] To directly test the utility of Gfi1 loss of function in leukemogenesis, *Mx1Cre*$^{+}$ mice with a *K-ras*$^{lsl G12D}$ gene and either wild-type or floxed *Gfi1* alleles (*Mx1Cre*$^{+}$ *K-ras*$^{lsl G12D}$ *Gfi1*$^{+/+}$ versus *Mx1Cre*$^{+}$ *K-ras*$^{lsl G12D}$ *Gfi1*$^{fex4\text{-}5/fex4\text{-}5}$) were injected with pIpC and monitored daily. Consistent with published reports,[35,36] induction of K-Ras^{G12D} expression resulted in a rapid, lethal MPD with a mean latency of 25 days (Figure 2E dotted line). However, although both genotypes lead to increased white blood cells in the peripheral blood (Figure 2F), *Mx1Cre*$^{+}$ *K-ras*$^{lsl G12D}$ *Gfi1*$^{fex4\text{-}5/fex4\text{-}5}$ mice displayed significantly decreased latency ($P < .01$) to approximately 16 days (Figure 2E solid line). Moreover, although K-Ras^{G12D} expression induced the expansion of differentiated myeloid lineage cells in the peripheral blood, *Mx1Cre*$^{+}$ *K-ras*$^{lsl G12D}$ *Gfi1*$^{fex4\text{-}5/fex4\text{-}5}$ phenotypes included abnormal blast cells in the peripheral blood ($P < .01$; Figure 2F). To validate the leukemogenic capacity of such blasts, splenic cells from killed mice of both experimental groups were transplanted into sublethally irradiated CD45.1 congenic recipients. In agreement with published reports,[35,36] cells from the spleen of *Mx1Cre*$^{+}$ *K-ras*$^{lsl G12D}$*Gfi1*$^{+/+}$ mice did not produce a phenotype in transplant recipients. In contrast, transplantation of cells from the spleen of *Mx1Cre*$^{+}$ *K-ras*$^{lsl G12D}$ *Gfi1*$^{fex4\text{-}5/fex4\text{-}5}$ mice induced an acutely lethal disease characterized by increased white blood cell (WBC) counts and the presence of circulating undifferentiated blasts within 2 weeks (Figure 2I). We conclude that Gfi1 loss of function induces the progression of the K-Ras^{G12D}–associated MPD to AML.

Gfi1 loss of function transcriptionally reprograms GMPs through HoxA9

We next wanted to determine whether the elevated levels of HoxA9, Pbx1, and Meis1 in *Gfi1*$^{-/-}$ Lin^{-} bone marrow cells resulted in functional transcriptional programming. Therefore, we examined confirmed HoxA9-target genes *c-Myb*, *CD34*, and *Pim1*,[11-13] as well as putative HoxA9 target genes *Flt3*, *Pu.1*, *Cxcr4*, and *Ebf1*.[37] We found that the steady-state levels of *c-Myb*, *Pim1*, *Pu.1*, and *Cxcr4* transcripts were significantly increased in *Gfi1*$^{-/-}$ compared with *Gfi1*$^{+/+}$ Lin^{-} bone marrow cells (Figure 3A). However, the level of *CD34*, *Flt3*, and *Ebf1* were not increased (Figure 3A). Given the disparity that some but not all HoxA9 target genes were up-regulated in the absence of Gfi1, we questioned whether Gfi1 directly regulates *HoxA9*, *Pbx1*, and *Meis1*. First, we performed ChIP on human myeloid leukemia cells to find binding to the promoter, but not the 3′ untranslated region of *HoxA9*, *Pbx1*, and *Meis1* (Figure 3B). Next, we knocked down Gfi1 expression in the same cell line, which ablated Gfi1 binding to all 3 genes (Figure 3B) and up-regulated endogenous *HoxA9* expression. We conclude that Gfi1 directly and specifically regulates *HoxA9*, *Pbx1*, and *Meis1*.

To reconcile the failure of Gfi1 loss of function to deregulate all HoxA9 target genes, we next examined CMPs and GMPs isolated from *ROSA-Cre-ER*$^{T2+}$ *Gfi1*$^{fex4\text{-}5/fex4\text{-}5}$ bone marrow cells cultured with or without OHT for the expression of *HoxA9*, *Pbx1*, and *Meis1*. Interestingly, although tamoxifen-activated Cre-mediated deletion of floxed *Gfi1* alleles induced the expression of *HoxA9* and *Pbx1* in both CMPs and GMPs, we noted that *Meis1* was induced only in GMPs (compare Figure 3C with 3D). The reason for *Meis1* induction in GMPs but not CMPs is not known, but it corresponds to the dramatic expansion of GMP on conditional *Gfi1* deletion (Figure 2D). We therefore reasoned that the disparity in transcriptional programming (Figure 3A) might be resolved in GMPs, where *Meis1* is significantly induced on*Gfi1* deletion (Figure 3D). Indeed, the expression of *c-Myb*, *CD34*, *Pim1*, *Flt3*, *Pu.1*, *Cxcr4*, and *Ebf1* were significantly increased in GMPs after conditional deletion of floxed *Gfi1* alleles (Figure 3E). We conclude that loss of Gfi1 transcriptionally reprograms GMPs.

Germline deletion of Hox genes can affect the regulation of surrounding genes.[38] Thus, it is formally possible that Gfi1 regulation of *HoxA9* could affect multiple nearby HoxA locus genes. Other than *HoxA9*, which was increased approximately 8-fold in *Gfi1*$^{-/-}$ Lin^{-} bone marrow cells (Figure 1C), we did not detect significant deregulation of other *HoxA* genes in Lin^{-} bone marrow cells (data not shown). Because Gfi1 loss of function affects progenitor numbers (which could skew gene expression changes) we refined our analyses to purified *Gfi1*$^{+/+}$ and *Gfi1*$^{-/-}$ GMPs. The steady-state levels of *HoxA9* transcripts were increased approximately 16-fold in purified GMPs (Figure 3F). Notably, other *HoxA* locus genes were not as dramatically deregulated (Figure 3F). Mouse *Gfi1*$^{-/-}$ and human GFI1N382S progenitors accumulate in vivo.[22,23,25] Thus, we next examined the level of *HOXA9* in GFI1N382S patient CD34^{+} bone marrow cells. Compared with 3 independent samples of normal CD34^{+} bone marrow cells, the level of *HoxA9* was induced 8-fold in the GFI1N382S sample (Figure 3G). Together, these data indicate that regulation of *HoxA9* by Gfi1 is specific and conserved.

We next analyzed the consequence of *HoxA9* loss to the in vitro phenotype mediated by Gfi1 dominant-negative mutants. We included *HoxA7*$^{-/-}$ mice in our analyses as a control for genetic manipulation of this locus. Wild-type, *HoxA7*$^{-/-}$, and *HoxA9*$^{-/-}$ Lin^{-} bone marrow cells were transduced with retroviral vectors expressing Gfi1 dominant-negative mutants (P2A or N382S) and were plated to analyze CFU capacity. Colonies were enumerated, and cells were serially plated until CFUs were exhausted. Although the expression of Gfi1 dominant-negative mutants in wild-type or *HoxA7*$^{-/-}$ bone marrow cells induced increased colony replating (Figure 3H), *HoxA9*$^{-/-}$ bone marrow cells were not responsive, with *HoxA9*$^{-/-}$ cells lacking CFUs after the third plating with or without Gfi1 dominant-negatives (Figure 3I). These data indicate that HoxA9 is critically required to induce the in vitro persistence of myeloid progenitors induced by Gfi1 loss of function.

Gfi1 and HoxA9 epistasis

Given these strong in vitro phenotypes, we next examined *Gfi1-HoxA9* epistasis in vivo by mating *Gfi1*$^{+/-}$ and *HoxA9*$^{+/-}$ mice to obtain *Gfi1*$^{+/-}$ *HoxA9*$^{+/-}$ progeny, which were then intercrossed to obtain mice with variable numbers of *Gfi1* and *HoxA9* alleles. Similar experiments with *HoxA7*$^{-/-}$ mice were performed as a control and show that altering HoxA7 alleles does not alter *Gfi1*$^{-/-}$ phenotypes. *Gfi1*$^{-/-}$ mice display increased GMPs and decreased megakaryocyte erythroid progenitors (MEPs). Limiting *HoxA9* alleles significantly decreased the number of *Gfi1*$^{-/-}$ GMPs (Figure

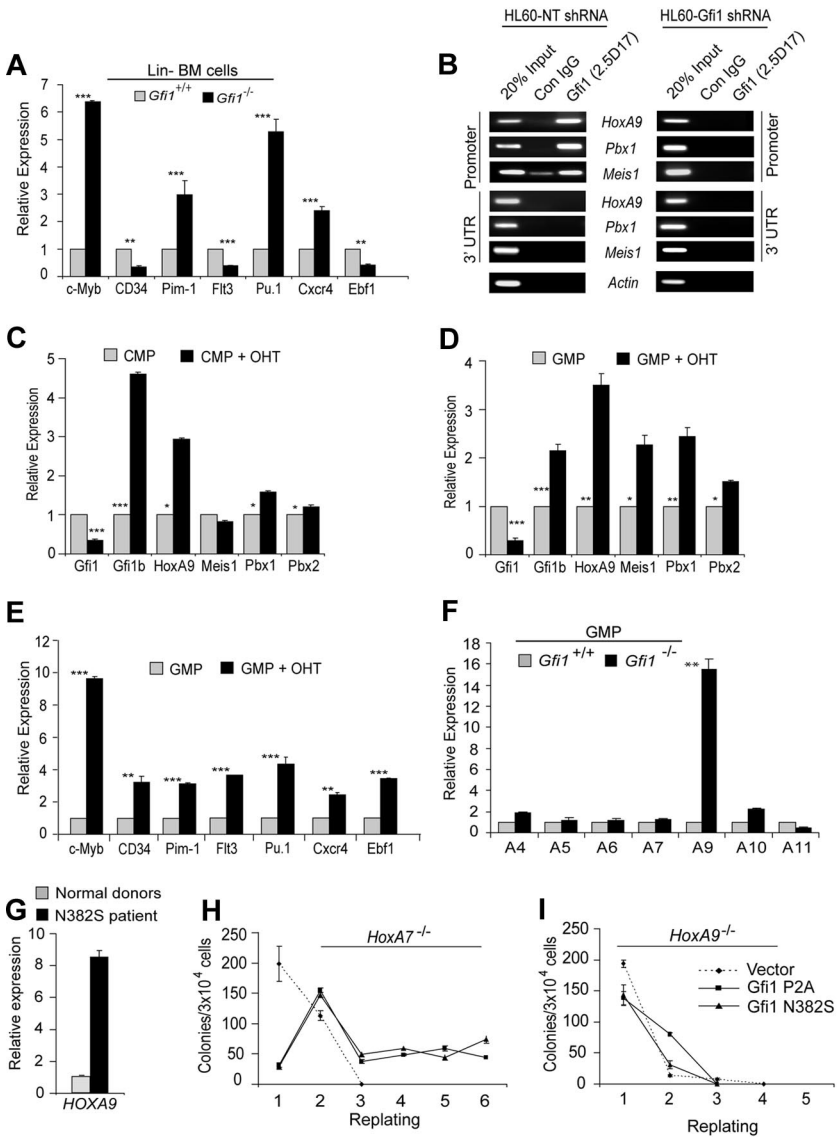

Figure 3. Gfi1 loss of function directly deregulates *HoxA9*, *Pbx1*, and *Meis1* in GMPs. (A) Quantitative real-time gene expression analysis of putative HoxA9-target genes *c-Myb*, *CD34*, *Pim1*, *Flt3*, *Pu.1*, *Cxcr4*, and *Ebf1* in RNA from wild-type or *Gfi1*$^{-/-}$ littermate Lin$^-$ bone marrow cells. (B) Chromatin immunoprecipitation (ChIP) analysis with a Gfi1-specific monoclonal antibody (2.5D.17) or isotype control IgG (Con IgG) showing Gfi1 physically bound to conserved promoter elements in *HoxA9*, *Pbx1*, and *Meis1* (Promoter), but not 3′-untranslated regions of these genes (3′UTR). Gfi1 binding was detected in control nontargeting shRNA-treated HL60 cells (HL60-NT shRNA) but not in Gfi1-specific shRNA-knock-down HL60 cells (HL60-Gfi1 shRNA). (C,D) Quantitative real-time gene expression analysis of *Gfi1*, *Gfi1b*, *HoxA9*, *Meis1*, *Pbx1*, and *Pbx2* in sorted CMPs (C) and GMPs (D) from *RosaCreER*$^{T2+}$ *Gfi1*$^{fex4\text{-}5/fex4\text{-}5}$ Lin$^-$ bone marrow cells with or without tamoxifen (OHT). (E) Quantitative real-time gene expression analysis of putative HoxA9-target genes *c-Myb, CD34, Pim1, Flt3, Pu.1, Cxcr4*, and *Ebf1* in RNA from panel D. (F) Quantitative real-time gene expression analysis of *HoxA* locus gene expression in RNA from wild-type or *Gfi1*$^{-/-}$ littermate isolated GMPs. (G) Quantitative real-time gene expression analysis of *HoxA9* in CD34$^+$ bone marrow cells from 3 healthy donors or a GFI1N382S patient. Error bars indicate SD. (H,I) Methylcellulose colony-forming assay with serial replating of *HoxA7*$^{-/-}$ (H) or *HoxA9*$^{-/-}$ (I) Lin$^-$ bone marrow cells transduced with retrovirus expressing Gfi1 dominant-negative mutants (P2A or N382S) or an empty vector control. Error bars indicate SEM.

4A,B) and increased the number of *Gfi1*$^{-/-}$ MEPs in a dose-dependent manner (Figure 4A). Moreover, the in vitro replating capacity of *Gfi1*$^{-/-}$ bone marrow cells was normalized by limiting even a single allele of *HoxA9* (Figure 4C). In vitro, we found that the number of *HoxA9* alleles correlated with the number of CFU-Ms, but that limiting *Gfi1* alleles increased *HoxA9*$^{-/-}$ CFU-Ms (Figure 4D). In contrast, limiting *HoxA9* alleles did not overcome the *Gfi1*$^{-/-}$ block to terminal differentiation of granulocytes in vitro (Figure 4D) or in vivo (Figure 4A). Similarly, we did not detect a statistically significant effect of limiting *HoxA9* alleles on the number of phenotypic short-term or long-term *Gfi1*$^{-/-}$ HSCs. We conclude that the in vivo and in vitro phenotypes of *Gfi1*$^{-/-}$ progenitors critically depend on *HoxA9*.

Interestingly, the *Gfi1*$^{-/-}$*HoxA9*$^{-/-}$ bone marrow displayed a striking differentiation defect indicated by the abundance of bone marrow cells with abnormal morphology (Figure 4A). Overall, the *Gfi1*$^{-/-}$*HoxA9*$^{-/-}$ bone marrow displayed poor colony formation with total CFU numbers typically 67% to 75% lower than either *Gfi1*$^{-/-}$ or *HoxA9*$^{-/-}$ single knockouts (Figure 4D). With CFU-Gs restricted by the lack of Gfi1, the constriction centered mainly on the loss of CFU-Ms (Figure 4D). Phenotypic *Gfi1*$^{-/-}$*HoxA9*$^{-/-}$ CMPs and GMPs were clearly present (Figure 4A), but they failed to efficiently form colonies (Figure 4C,D). Moreover, the colonies that did form were completely devoid of secondary replating capacity (Figure 4C). Thus, the *Gfi1*$^{-/-}$*HoxA9*$^{-/-}$ mice died within 1 month of birth and displayed compounded defects similar to a bone marrow failure syndrome.

Discussion

Gfi1 integrates myeloid progenitor quiescence and differentiation through separable transcriptional programs. Patients with GFI1N382S SCN display the accumulation of differentiation-arrested myeloid progenitors.[25] Similarly, *Gfi1*$^{-/-}$ mice exhibit an accumulation of GMPs and abnormal arrested progenitors,[22,23] associated with increased stem and progenitor proliferation.[24,39] However, the underlying molecular mechanisms have not been described. Gfi1 loss of function through germline *Gfi1* deletion leads to the accumulation of GMPs in vivo.[22,23] This phenotype

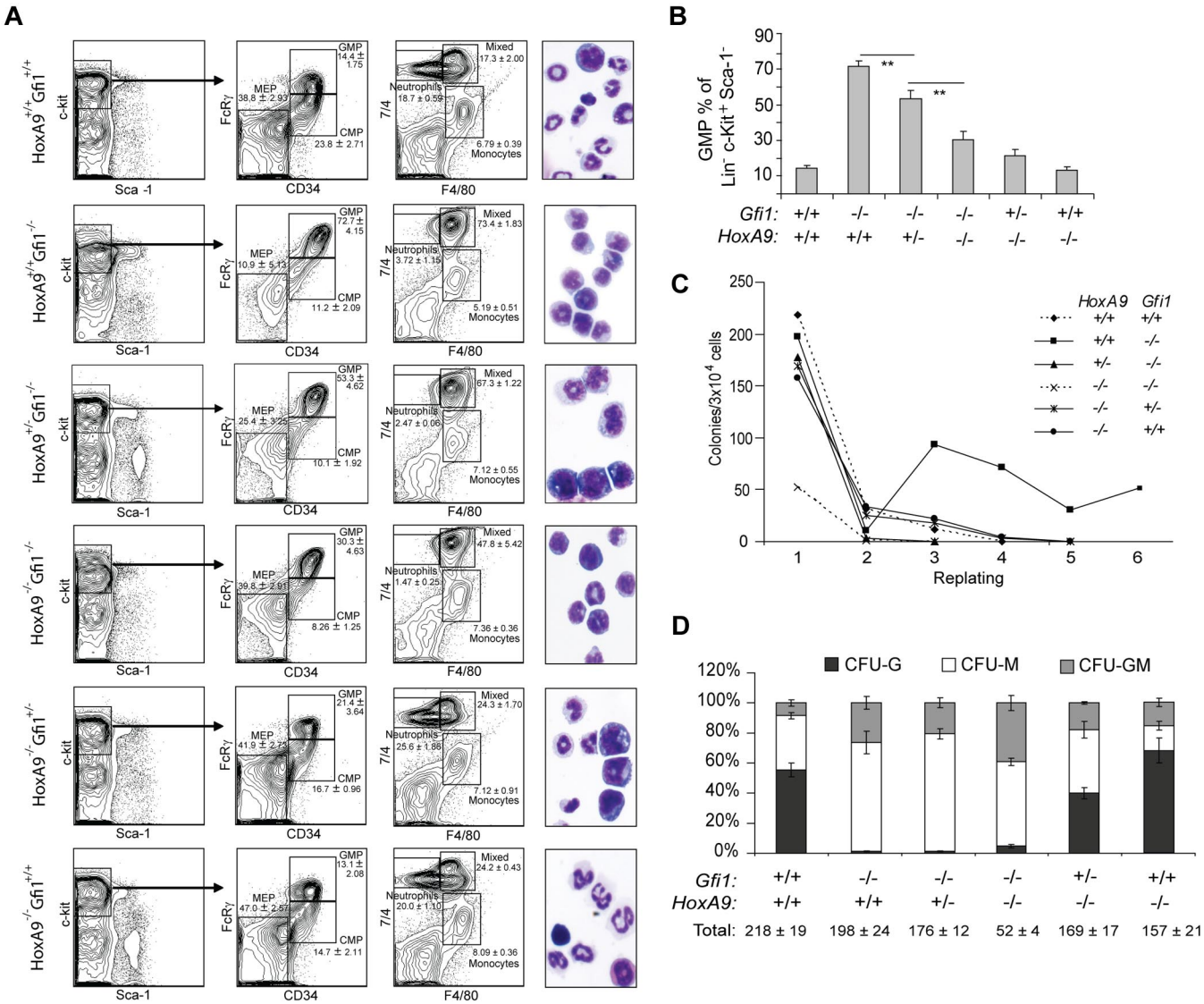

Figure 4. HoxA9 controls Gfi1-induced myeloid progenitor differentiation, in vivo accumulation, and in vitro life span. (A) Flow cytometric analyses of bone marrow cells from mice (WT, n = 4; *HoxA9*$^{-/-}$*Gfi1*$^{+/+}$, n = 4; *HoxA9*$^{-/-}$*Gfi1*$^{+/-}$, n = 4; *HoxA9*$^{-/-}$*Gfi1*$^{-/-}$, n = 4; *HoxA9*$^{+/-}$*Gfi1*$^{-/-}$, n = 2; *HoxA9*$^{+/+}$*Gfi1*$^{-/-}$, n = 4). Populations ± SD (insets) are shown. Photomicrographs (×100) of cytospins from whole bone marrow preparations of representative animals (right). (B) Graphic representation of GMP in panel A. (C) Methylcellulose serial replating assay of Lin$^-$ bone marrow cells from mice in panel A. (D) Methylcellulose colony formation assays of bone marrow cells with percentages displayed are the average of independent analyses from individual mice in panel A. All assays represented (A-D) were initiated from 1 cohort of mice on the same day. Results shown are representative of at least 3 separate analyses on different cohorts. Error bars indicate SEM. $^{**}P \leq .01$

correlates to an extended ability to form colonies in vitro induced by *Gfi1* deletion or the expression of SCN-associated Gfi1 dominant-negative mutants, which shows that the phenotype is cell autonomous. The molecular mechanism pivots on Gfi1 regulation of the activity and expression of the HoxA9-Pbx1-Meis1 transcription factor complex, which is normally suppressed by Gfi1 during myeloid progenitor differentiation. Failure to induce the Gfi1 program in GMPs deregulates transcriptional control of normal hematopoietic progenitors and leads to their accumulation, but this can be uncoupled from a failure to form granulocytes.

Gfi1 directly regulates the HoxA9-Pbx1-Meis1 transcription factor complex in myeloid progenitors. First, Gfi1 binds to evolutionarily conserved elements in the promoters of the *HoxA9, Pbx1*, and *Meis1* genes in living cells (Figure 5B). The binding results in functional gene regulation because the expression of *Gfi1* is inverse to *HoxA9*, *Pbx1*, and *Meis1* expression during the normal transition from CMPs to GMPs. Moreover, *HoxA9, Pbx1*, and *Meis1* expression is induced on conditional deletion of *Gfi1* in GMPs. In contrast, forced expression of Gfi1 lowers *HoxA9*, *Pbx1*, and *Meis1* expression in wild-type cells and rescues *HoxA9*, *Pbx1*, and *Meis1* expression in *Gfi1*$^{-/-}$ cells. In the absence of Gfi1, *HoxA9* autoregulation[40] may further elevate HoxA9 expression levels. Thus, Gfi1 represses *Pbx1* and *Meis1* and competes with HoxA9 autoregulation to control *HoxA9*. The normal physiologic context of Gfi1 versus HoxA9-Pbx1-Meis1 antagonism is the CMP-to-GMP transition in which the induction of Gfi1 directly represses the continued expression of HoxA9-Pbx1-Meis1 factors (Figure 5).

SCN phenotypes induced by GFI1 loss of function may derive from deregulation of myelopoiesis at multiple points. Notably, HoxA9-dependent transcriptional programming modulates myeloid differentiation, but lowering HoxA9 alleles in *Gfi1*$^{-/-}$ progenitors

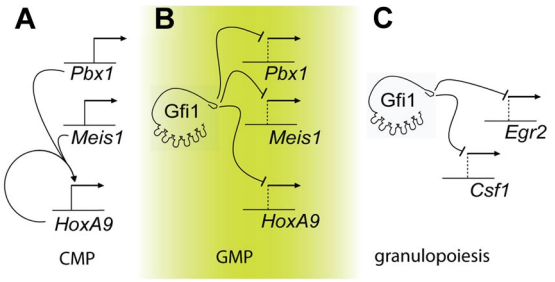

Figure 5. Gfi1 integrates separable transcriptional programs in myeloid progenitors. Graphic representations. (A) In CMPs, *HoxA9* is autoregulated. (B) In GMPs, Gfi1 represses *Meis1*, *Pbx1*, and *HoxA9*. Deregulation of Gfi1 leads to the HoxA9-dependent accumulation of myeloid progenitors. (C) Granulopoiesis is critically controlled by Gfi1 repression of target genes such as *Csf1* and *Egr2*.[20,47]

does not permit terminal granulopoiesis. In contrast, we have recently shown that the deregulation of *Csf1* by SCN-associated Gfi1 mutants is critical to the Gfi1 loss-of-function impairment of terminal granulopoiesis (Figure 5).[20] Therefore, multiple steps in myeloid development may be controlled by Gfi1 and deregulated in patients with *GFI1*-mutant SCN. First, the ability to induce terminal granulopoietic transcriptional programming is blocked by monopoietic signaling from Csf1[20] (Figure 5C). Second, elevated expression of *HoxA9, Pbx1*, and *Meis1*, which should normally be down-regulated during the transition from CMPs to GMPs (Figure 5A,B), induces the abnormal accumulation of arrested myeloid progenitors. In Gfi1-null mice, such cells express primary granule genes such as *MPO* and *ELA2*.[23] In ex vivo culture systems, forced expression of HoxA9 and Meis1 in primary murine bone marrow cells transform G-CSF stimulation into a proliferative signal.[41] We note that recombinant G-CSF therapy for patients with GFI1-mutant SCN further expands arrested myeloid progenitors to mediate modest protection from infection.[25] Thus, our data provide a potential explanation for this clinical observation.

HoxA9 activity is critical to the $Gfi1^{-/-}$ deregulation of progenitor biology but not granulopoiesis. Gfi1 loss of function increases GMP numbers but blocks terminal granulopoiesis in vivo and CFU-Gs in vitro.[20,22,23] HoxA9 loss of function lowers CMP numbers (but not GMP) in vivo[4] and decreases CFU-Ms in vitro. $Gfi1^{-/-}$ GMPs show an approximate 16-fold induction of *HoxA9* expression. In experiments to examine epistasis, limiting alleles of *HoxA9* lowered the number of $Gfi1^{-/-}$ GMPs and increased the number of $Gfi1^{-/-}$ MEPs in vivo. These results are underscored by the dose-dependent relationship between *HoxA9* alleles and $Gfi1^{-/-}$ GMP accumulation. In vitro, limiting *HoxA9* alleles eliminated $Gfi1^{-/-}$ colony replating, showing that the in vitro persistence of $Gfi1^{-/-}$ colony-forming cells critically depends on HoxA9. Thus, these $Gfi1^{-/-}$ phenotypes are hypostatic to *HoxA9*. Because lack of Gfi1 prevented the formation of CFU-Gs in vitro and granulocytes in vivo (independent of *HoxA9* status), *HoxA9* and *Gfi1* epistasis is not a critical factor in terminal granulopoiesis. One might consider that myeloid progenitors that are unable to differentiate may accumulate as a default; however, we conclude that $Gfi1^{-/-}$ progenitor accumulation (but not terminal granulopoiesis) is controlled by *HoxA9*.

As evidenced by dramatic expansion of CFUs after inducible *Gfi1* deletion in isolated cells in vitro, the expansion of $Gfi1^{-/-}$ GMPs in vivo is most likely due to the abnormal proliferative potential of such cells. We note that the forced expression of Gfi1 dominant negatives and conditional *Gfi1* deletion amplify an expansion of CFUs, followed by a contraction to replatable colonies. We speculate that the differentiation state of the progenitors may control the response to loss of *Gfi1*. Specifically, deregulation of *Meis1* appeared to be specific to GMPs, and *Meis1* responded differently to Gfi1 expression in both $Gfi1^{+/+}$ and $Gfi1^{-/-}$ Lin^- cells compared with *HoxA9* and *Pbx1*. In vitro, $Gfi1^{-/-}$ marrow has been reported to be hyperresponsive to cytokines,[22,23] providing a potential explanation for $Gfi1^{-/-}$ progenitor proliferation. However, these observations were based on total CFUs generated by whole bone marrow and did not accommodate the dramatic changes in progenitor numbers within $Gfi1^{-/-}$ marrow. $HoxA9^{-/-}$ marrow does not display differential cytokine sensitivity.[4] $Gfi1^{-/-}$ GMPs display dramatic deregulation of *HoxA9* expression. We note that the in vivo accumulation of $Gfi1^{-/-}$ GMPs and the in vitro colony replating effect of Gfi1 loss of function are dependent on *HoxA9* dosage. In $Gfi1^{+/+}$ cells, HoxA9 overexpression induces progenitor proliferation.[3] Thus, it is most likely that the proliferative response of isolated progenitors to Gfi1 loss is due to deregulation of HoxA9 and not to cytokine hypersensitivity.

The profound phenotype of $Gfi1^{-/-}HoxA9^{-/-}$ hematopoietic cells highlights the importance of Gfi1 versus HoxA9 transcriptional programming. Loss of both factors in $Gfi1^{-/-}HoxA9^{-/-}$ mice lead to the presence of abnormal bone marrow cells, decreased total CFUs, and survival. Similar to $HoxA9^{-/-}$ phenotypic HSCs,[42] the numbers of $Gfi1^{-/-}HoxA9^{-/-}$ phenotypic CMP and GMP progenitors did not correlate to biologic capacity, indicating that such cells are biologically defective. Moreover, $Gfi1^{-/-}HoxA9^{-/-}$ phenotypes are more profound than deletion of either *Gfi1* or *HoxA9* alone[24,42] and are similar to a bone marrow failure syndrome.

Although Gfi1 is one of the most common genes affected by Moloney leukemia virus (MoMLV) integration in lymphoid leukemias,[16] it is rarely seen in myeloid leukemias driven by MoMLV-derivative viruses.[43] The reason that insertions in Gfi1 are infrequently seen in myeloid tumors is explained by its repression of HoxA9, Pbx1, and Meis1, which are required for progenitor immortalization and expansion. In mice, the activation of oncogenic Ras (and subsequent chronic Map-kinase signaling) leads to both a proliferative and a differentiation stimulus and lethal overproduction of mature myeloid cells.[44] Gfi1-Ras leukemogenesis is probably explained by a $Gfi1^{-/-}$ block to Ras-Map-kinase–induced differentiation within self-renewing cells, which also gain $Gfi1^{-/-}$ proliferative potential. Key molecules that antagonize transformation represent attractive candidates for clinical intervention in leukemia and myeloproliferative disorders. Therefore, the transcriptional programs controlled by Gfi1 are attractive targets for manipulation in such diseases.

In sum, the data show that the transcriptional program initiated by a single transcription factor (Gfi1) integrates myeloid lineage differentiation and proliferation by antagonizing HoxA9-Pbx1-Meis1 activity. This integrative function of Gfi1 is similar to the activity of c-Myc that simultaneously stimulates both cell-cycle progression and exposure to apoptosis.[45] Although transcription factor pairs such as C/EBPα/Fog1, C/EBPα/Pu.1, Pu.1/Gfi1, and Eklf/Fli are known to antagonize each other to regulate lineage fate decisions,[46-49] the transcriptional antagonism mediated by Gfi1 and HoxA9 is unique in that it includes autoregulation and the integration of separable transcriptional programs controlling progenitor life span and differentiation.

Acknowledgments

We thank Christopher Baum and Axel Schambach for the SF91 vector, Jonathan Walsh for the CMMP vectors, Anton Berns for the ROSA-Cre-ERt2 mice, and Michael A. Caligiuri for HoxA9$^{-/-}$ and HoxA7$^{-/-}$ mice. We also thank Michelle Meadows and Avinash Baktula for technical assistance and James Phelan, Brian Gebelein, Anil Jegga, Chris Karp, Jose Cancelas, Jim Mulloy, and Hartmut Geiger for scientific discussions.

This work was supported by the Division of Intramural Research, NIAID, NIH (J.Z. and W.E.P.), by a grant from Cancerfree Kids (Loveland, OH), and by NIH (CA105152 and HL079574; H.L.G.).

Authorship

Contribution: S.R.H. and C.S.V. designed and performed experiments, analyzed results, generated figures, and wrote the paper; T.B. performed flow cytometry; J.Z. and W.E.P. provided mice; A.C. performed leukemogenesis experiments; B.G. provided essential conceptual information and data before publication; and H.L.G. designed experiments and wrote the paper.

Conflict-of-interest disclosure: The authors declare no competing financial interests.

Correspondence: H. Leighton Grimes, Division of Immunobiology, Cincinnati Children's Hospital Medical Center, 3333 Burnet Ave MLC7038, Cincinnati, OH 45229; e-mail: lee.grimes@cchmc.org

References

1. Abramovich C, Humphries RK. Hox regulation of normal and leukemic hematopoietic stem cells. Curr Opin Hematol. 2005;12:210-216.
2. Grier DG, Thompson A, Kwasniewska A, McGonigle GJ, Halliday HL, Lappin TR. The pathophysiology of HOX genes and their role in cancer. J Pathol. 2005;205:154-171.
3. Thorsteinsdottir U, Mamo A, Kroon E, et al. Overexpression of the myeloid leukemia-associated Hoxa9 gene in bone marrow cells induces stem cell expansion. Blood. 2002;99:121-129.
4. Lawrence HJ, Helgason CD, Sauvageau G, et al. Mice bearing a targeted interruption of the homeobox gene HOXA9 have defects in myeloid, erythroid, and lymphoid hematopoiesis. Blood. 1997;89:1922-1930.
5. Shen WF, Montgomery JC, Rozenfeld S, et al. AbdB-like Hox proteins stabilize DNA binding by the Meis1 homeodomain proteins. Mol Cell Biol. 1997;17:6448-6458.
6. Shen WF, Rozenfeld S, Kwong A, Köm ves LG, Lawrence HJ, Largman C. HOXA9 forms triple complexes with PBX2 and MEIS1 in myeloid cells. Mol Cell Biol. 1999;19:3051-3061.
7. Rieckhof GE, Casares F, Ryoo HD, Abu-Shaar M, Mann RS. Nuclear translocation of extradenticle requires homothorax, which encodes an extradenticle-related homeodomain protein. Cell. 1997;91:171-183.
8. Berthelsen J, Kilstrup-Nielsen C, Blasi F, Mavilio F, Zappavigna V. The subcellular localization of PBX1 and EXD proteins depends on nuclear import and export signals and is modulated by association with PREP1 and HTH. Genes Dev. 1999; 13:946-953.
9. Pai CY, Kuo TS, Jaw TJ, et al. The homothorax homeoprotein activates the nuclear localization of another homeoprotein, extradenticle, and suppresses eye development in Drosophila. Genes Dev. 1998;12:435-446.
10. Kirito K, Fox N, Kaushansky K. Thrombopoietin induces HOXA9 nuclear transport in immature hematopoietic cells: potential mechanism by which the hormone favorably affects hematopoietic stem cells. Mol Cell Biol. 2004;24:6751-6762.
11. Wang GG, Pasillas MP, Kamps MP. Persistent transactivation by meis1 replaces hox function in myeloid leukemogenesis models: evidence for co-occupancy of meis1-pbx and hox-pbx complexes on promoters of leukemia-associated genes. Mol Cell Biol. 2006;26:3902-3916.
12. Hess JL, Bittner CB, Zeisig DT, et al. c-Myb is an essential downstream target for homeobox-mediated transformation of hematopoietic cells. Blood. 2006;108:297-304.
13. Hu YL, Passegue E, Fong S, Largman C, Lawrence HJ. Evidence that the Pim1 kinase gene is a direct target of HOXA9. Blood. 2007; 109:4732-4738.
14. Gilks CB, Bear SE, Grimes HL, Tsichlis PN. Progression of interleukin-2 (IL-2)-dependent rat T cell lymphoma lines to IL-2-independent growth following activation of a gene (Gfi-1) encoding a novel zinc finger protein. Mol Cell Biol. 1993;13: 1759-1768.
15. Scheijen B, Jonkers J, Acton D, Berns A. Characterization of pal-1, a common proviral insertion site in murine leukemia virus-induced lymphomas of c-myc and Pim-1 transgenic mice. J Virol. 1997;71:9-16.
16. Uren AG, Kool J, Matentzoglu K, et al. Large-scale mutagenesis in p19(ARF)- and p53-deficient mice identifies cancer genes and their collaborative networks. Cell. 2008;133:727-741.
17. Grimes HL, Chan TO, Zweidler-McKay PA, Tong B, Tsichlis PN. The Gfi-1 proto-oncoprotein contains a novel transcriptional repressor domain, SNAG, and inhibits G1 arrest induced by interleukin-2 withdrawal. Mol Cell Biol. 1996;16: 6263-6272.
18. Zweidler-Mckay PA, Grimes HL, Flubacher MM, Tsichlis PN. Gfi-1 encodes a nuclear zinc finger protein that binds DNA and functions as a transcriptional repressor. Mol Cell Biol. 1996;16: 4024-4034.
19. Fiolka K, Hertzano R, Vassen L, et al. Gfi1 and Gfi1b act equivalently in haematopoiesis, but have distinct, non-overlapping functions in inner ear development. EMBO Rep. 2006;7:326-333.
20. Zarebski A, Velu CS, Baktula AM, et al. Mutations in growth factor independent-1 associated with human neutropenia block murine granulopoiesis through colony stimulating factor-1. Immunity. 2008;28:370-380.
21. Zhu J, Guo L, Min B, et al. Growth factor independent-1 induced by IL-4 regulates Th2 cell proliferation. Immunity. 2002;16:733-744.
22. Karsunky H, Zeng H, Schmidt T, et al. Inflammatory reactions and severe neutropenia in mice lacking the transcriptional repressor Gfi1. Nat Genet. 2002;30:295-300.
23. Hock H, Hamblen MJ, Rooke HM, et al. Intrinsic requirement for zinc finger transcription factor Gfi-1 in neutrophil differentiation. Immunity. 2003; 18:109-120.
24. Hock H, Hamblen MJ, Rooke HM, et al. Gfi-1 restricts proliferation and preserves functional integrity of haematopoietic stem cells. Nature. 2004;431:1002-1007.
25. Person RE, Li FQ, Duan Z, et al. Mutations in proto-oncogene GFI1 cause human neutropenia and target ELA2. Nat Genet. 2003;34:308-312.
26. Li-Kroeger D, Witt LM, Grimes HL, Cook TA, Gebelein B. Hox and senseless antagonism functions as a molecular switch to regulate EGF secretion in the Drosophila PNS. Dev Cell. 2008;15: 298-308.
27. Zhu J, Jankovic D, Grinberg A, Guo L, Paul WE. Gfi-1 plays an important role in IL-2-mediated Th2 cell expansion. Proc Natl Acad Sci U S A. 2006; 103:18214-18219.
28. Chen F, Greer J, Capecchi MR. Analysis of Hoxa7/Hoxb7 mutants suggests periodicity in the generation of the different sets of vertebrae. Mech Dev. 1998;77:49-57.
29. Fromental-Ramain C, Warot X, Lakkaraju S, et al. Specific and redundant functions of the paralogous Hoxa-9 and Hoxd-9 genes in forelimb and axial skeleton patterning. Development. 1996; 122:461-472.
30. Hameyer D, Loonstra A, Eshkind L, et al. Toxicity of ligand-dependent Cre recombinases and generation of a conditional Cre deleter mouse allowing mosaic recombination in peripheral tissues. Physiol Genomics. 2007;31:32-41.
31. Akashi K, Traver D, Miyamoto T, Weissman IL. A clonogenic common myeloid progenitor that gives rise to all myeloid lineages. Nature. 2000;404: 193-197.
32. Kroon E, Krosl J, Thorsteinsdottir U, Baban S, Buchberg AM, Sauvageau G. Hoxa9 transforms primary bone marrow cells through specific collaboration with Meis1a but not Pbx1b. EMBO J. 1998;17:3714-3725.
33. Thorsteinsdottir U, Krosl J, Kroon E, Haman A, Hoang T, Sauvageau G. The oncoprotein E2A-Pbx1a collaborates with Hoxa9 to acutely transform primary bone marrow cells. Mol Cell Biol. 1999;19:6355-6366.
34. Chan IT, Gilliland DG. Oncogenic K-ras in mouse models of myeloproliferative disease and acute myeloid leukemia. Cell Cycle. 2004;3:536-537.
35. Braun BS, Tuveson DA, Kong N, et al. Somatic activation of oncogenic Kras in hematopoietic cells initiates a rapidly fatal myeloproliferative disorder. Proc Natl Acad Sci U S A. 2004;101:597-602.
36. Chan IT, Kutok JL, Williams IR, et al. Conditional expression of oncogenic K-ras from its endogenous promoter induces a myeloproliferative disease. J Clin Invest. 2004;113:528-538.
37. Wang GG, Pasillas MP, Kamps MP. Meis1 programs transcription of FLT3 and cancer stem cell character, using a mechanism that requires interaction with Pbx and a novel function of the Meis1 C-terminus. Blood. 2005;106:254-264.
38. Branford WW, Benson GV, Ma L, Maas RL, Potter SS. Characterization of Hoxa-10/Hoxa-11 transheterozygotes reveals functional redundancy and regulatory interactions. Dev Biol. 2000;224:373-387.

39. Zeng H, Yucel R, Kosan C, Klein-Hitpass L, Moroy T. Transcription factor Gfi1 regulates self-renewal and engraftment of hematopoietic stem cells. EMBO J. 2004;23:4116-4125.

40. Trivedi CM, Patel RC, Patel CV. Differential regulation of HOXA9 expression by nuclear factor kappa B (NF-kappaB) and HOXA9. Gene. 2008; 408:187-195.

41. Calvo KR, Knoepfler PS, Sykes DB, Pasillas MP, Kamps MP. Meis1a suppresses differentiation by G-CSF and promotes proliferation by SCF: potential mechanisms of cooperativity with Hoxa9 in myeloid leukemia. Proc Natl Acad Sci U S A. 2001;98:13120-13125.

42. Lawrence HJ, Christensen J, Fong S, et al. Loss of expression of the Hoxa-9 homeobox gene impairs the proliferation and repopulating ability of hematopoietic stem cells. Blood. 2005;106:3988-3994.

43. Akagi K, Suzuki T, Stephens RM, Jenkins NA, Copeland NG. RTCGD: retroviral tagged cancer gene database. Nucleic Acids Res. 2004;32: D523-527.

44. Orford KW, Scadden DT. Deconstructing stem cell self-renewal: genetic insights into cell-cycle regulation. Nat Rev Genet. 2008;9:115-128.

45. Evan G, Harrington E, Fanidi A, Land H, Amati B, Bennett M. Integrated control of cell proliferation and cell death by the c-myc oncogene. Philos Trans R Soc Lond B Biol Sci. 1994;345:269-275.

46. Dahl R, Iyer SR, Owens KS, Cuylear DD, Simon MC. The transcriptional repressor GFI-1 antagonizes PU. 1 activity through protein-protein interaction. J Biol Chem. 2007;282:6473-6483.

47. Laslo P, Spooner CJ, Warmflash A, et al. Multilineage transcriptional priming and determination of alternate hematopoietic cell fates. Cell. 2006; 126:755-766.

48. Querfurth E, Schuster M, Kulessa H, et al. Antagonism between C/EBPbeta and FOG in eosinophil lineage commitment of multipotent hematopoietic progenitors. Genes Dev. 2000;14:2515-2525.

49. Starck J, Cohet N, Gonnet C, et al. Functional cross-antagonism between transcription factors FLI-1 and EKLF. Mol Cell Biol. 2003;23:1390-1402.